J Mol Model (2003) 9:142–152
DOI 10.1007/s00894-003-0120-6

ORIGINAL PAPER

Ke-Cheng Wei · Han Zhou · Hao Wen · Wei Xu · Zhi-Hong Xu

Molecular mechanics and dynamics simulations of various dispersant models on the water surface (001)

Received: 17 September 2002 / Accepted: 22 January 2003 / Published online: 29 March 2003

Abstract Five dispersant-molecule models of succinimide, acrylate, imide, phenylsulfonic and salicyl were used to study their interactions with the water surface (001). The interaction energy, molecular configuration, charge distribution and radial distribution function (RDF) curve for each of the dispersant molecules were analyzed from the molecular mechanics (MM) and molecular dynamics (MD) simulation results. It can be seen that the system energies, mostly electrostatic and hydrogen bond energies, were reduced significantly when the dispersant molecules interacted with the water surface. The hydrophilic group of a dispersant molecule can attach itself to the water surface firmly and reach for a stable energy-minimized configuration, which is helpful to the dispersants' dispersancy. The influence exerted by the hydrophobic group of the dispersant molecule, which was the substituted hydrocarbon chain of *n*-octadecanyl in this paper, is discussed in comparison with the *naked polar headgroup*. Steric configuration, charge distribution and substitute hydrocarbon chain of the dispersant molecule influenced the interaction between dispersants and polar water surface.

Keywords Dispersant · Molecular mechanics · Molecular dynamics

Introduction

Dispersants are among the most important additives for lubricant oils. Their function is to prevent deleterious sludge accumulation on engine parts. The performances of lubricant dispersants are being optimized to cope with increased sludge formation resulting from enhanced thermal and oxidative degradation of lubricant formulations for today's hotter and faster-running engines. A typical dispersant is a combination of hydrophobic and hydrophilic moieties. It adsorbs on the surface of sludge particles to impede their further accumulation. As a complex colloidal system, the stabilization of lubricant oil has a direct relationship with the dispersancy of the dispersant, which depends on the chemical nature of the dispersant, the particle and the solvent. [1, 2, 3, 4, 5]

The experimental studies reported in [1] and [2] used the Langmuir trough method to investigate the molecular geometry and composition of the dispersant on the interfacial properties between succinimide and water surface. It can be concluded from these experiments that the polarity of the sludge or soot particle is an important factor in determining the dispersancy mechanism. Further aggregation of the particles to larger agglomerates would be hindered as the hydrophilic moiety of the dispersant molecules attached itself to their polar surface. However, detailed discussions on the influencing factors from their molecular structures and the relationship between the molecular structures and the performance of the dispersants were not given.

Understanding the mechanism of the complex physical and chemical interactions that occur between dispersant molecules and the sludge particles can help develop more efficient lubricant-oil dispersants. Molecular simulation techniques can clearly provide valuable insight into the molecular structure and performance of materials and model virtual experiments, which are difficult to perform physically, such as the dynamics process [6, 7, 8] and interface phenomena. [9, 10, 11, 12, 13, 14, 15] Among the various molecular simulation methods, molecular mechanics (MM) has been and still is appreciated as an approach that can optimize structures with high accuracy at comparatively little computational expense. [16] Fast and accurate calculation of structures for appreciably large molecules, extensive conformational search, dynamic processes, the interaction between isolated molecules and the environment are the aims of molecular

K.-C. Wei (✉) · H. Wen · Z.-H. Xu
Institute of Process Engineering,
Chinese Academy of Sciences,
Zhongguancun, P.O. Box 353, 100080 Beijing, China
e-mail: kchwei@lcc.icm.ac.cn

H. Zhou · W. Xu
SINOPEC Research Institute of Petroleum Processing,
18 Xueyuan Road, 100083 Beijing, China

dynamics (MD) studies. In the MM or MD methods, the energy of a molecule is decomposed into various valence energies, including bond, angle, torsion, inversion energies or any other cross terms, and non-bond energies, e.g., van der Waals, electrostatic and hydrogen bond energies.

In view of the above, MM and MD calculations were carried out in this paper to study the interaction between dispersants and the polar surface of particles and to find out the factors that influence the dispersancy mechanism.

Simulation procedures

Model molecules

Five hydrophilic groups, succinimide, [17] acrylate, [18] imide, phenylsulfonic and salicyl, were taken as the hydrophilic moiety of the dispersants in this study. Linear *n*-octadecanyl was taken as the hydrophobic moiety in order to simplify the molecular structures of the dispersants. The molecular structures of the dispersants are shown in Fig. 1, where the derivative R is n-$C_{18}H_{35}$. Five corresponding molecules without R-substitutes, called *naked polar headgroups* in this paper, were built for comparative analysis. It is obvious that three of the dispersants in Fig. 1 are ashless dispersants and the other two are non-ashless in general. The model molecules, the dispersant molecules in Fig. 1 and the corresponding naked polar headgroups were built using the 3D-Sketcher module in Cerius2 software.

In the microenvironment, one dispersant molecule, and especially its hydrophobic moiety, is assumed to interact with an infinite water surface. Prior to performing MD simulations, MM energy minimizer and charge equilibrium calculations should be performed. The MD simulations can be performed by placing each of the dispersant molecules on the water surface.

The water surface, taken as a model for polar solid materials, was used to interact with dispersants as in the experimental study in [1] and [2]. Figure 2 shows the top view of the water surface (001) frame, which was composed of 25×14×4 water molecules by the surface-builder module in Cerius2. The water molecules were kept unmoved in order to check the influence of the surface and reduce the worthless calculations when the MM or MD simulations were performed. The charge equilibrium calculations for water molecules before MD simulations showed that the charges of the hydrogen and oxygen atoms are 0.3500 and 0.7000, respectively.

Molecular mechanics and molecular dynamics simulation

Force field employed

The Dreiding 2.21 force field, a pure diagonal force field with harmonic valence terms and a cosine-Fourier expansion torsion term, was employed in the MM and MD simulations. The umbrella functional form was used

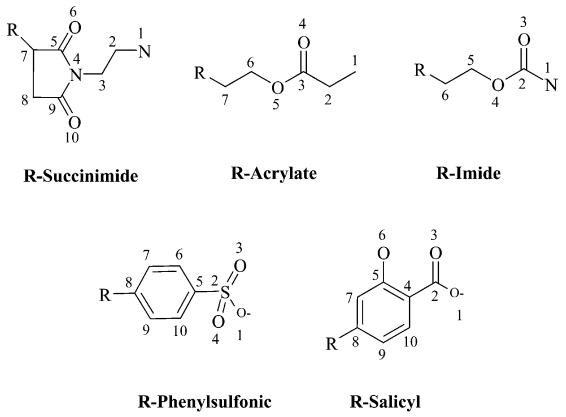

Fig. 1 Molecular structures of the dispersants

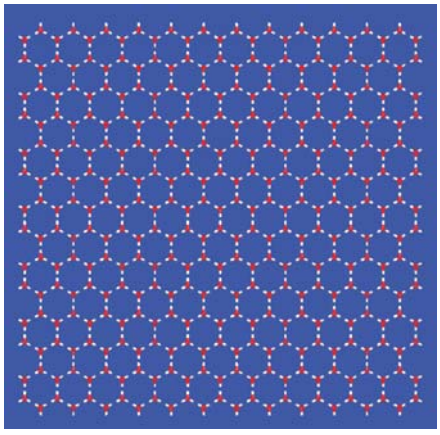

Fig. 2 Top view of the water surface (001)

for inversions, in accordance with the Wilson out-of-plane definition. The van der Waals interactions were described by the Lennard-Jones potential. Electrostatic interactions were described by atomic monopoles and a screened (distance-dependent) Coulombic term. Hydrogen bonding was described by an explicit Lennard-Jones 12–10 potential.

The Dreiding force field set automatically the type of the force field for the model molecules as listed in Table 1 when energy minimizer calculations were performed.

Geometry optimization

Geometry optimization was performed using the Truncated Newton algorithm in vacuo with a termination root mean square (RMS) gradient of 0.042 kJ mol^{-1} $Å^{-1}$ (0.01 kcal mol^{-1} $Å^{-1}$). Charge equilibrium calculations were performed using the Charge-Equilibration method with convergence criterion of 5.0×10^{-4}.

Table 1 Force field types for the dispersant molecules

Molecule	Atom	Force field type	Molecule	Atom	Force field type
Water	O	O_3	Imide	O	O_2
	H	H___A		O	O_R
C_{18}-hydrocarbon	C	C_3		N	N_3
	H	H_		H	H___A
Succinimide	O	O_2	Phenylsulfonic	O	O_2
	N (ring)	N_R		O (hydroxyl)	O_R
	N (amido)	N_3		H	H___A
	H (amido)	H___A	Salicyl	O	O_2
Acrylate	O (carbonyl)	O_2		S	S_3
	O	O_R			

Interactions between dispersants and water surface (001)

The MD simulations were performed by placing each of the dispersant molecules on the center region of the water surface (001) in the case that the geometry optimizations for dispersant molecules and charge equilibrium calculations for water molecules were completed.

The NVT ensemble was chosen in the MD simulations. One of the difficulties of the MD simulation is that the initial configuration of models has a direct influence on the final simulation results. The molecules will remain trapped in a local energy minimum when the temperature is low. In this work, the MD simulations were first performed at the temperature of 500 K with 20,000 steps to guarantee that the molecules can pass over the energy barriers. From the MD simulation results at 500 K, a most stable configuration with lowest energy can be picked as the starting configuration for the next MD simulations at lower temperatures. The final MD results were collected at a temperature of 300 K after 20,000 steps of MD simulation, which were enough to reach the state of dynamic equilibrium and meaningful statistics because only the dispersant molecule moved during the calculation.

The equations of motion were solved using the summed Verlet algorithm. Long-range interactions were calculated as spline sums, which are the best fit for nonperiodic models. Spline line on length was 11 Å, line off length 14 Å.

Results and discussion

In this paper, the aim of the MD simulations was to find what factors will influence the interaction between the dispersants and the water surface (001).

While observing the dynamic process of the dispersant molecules on the water surface (001), the phenomenon was discovered that the hydrophilic groups of all those molecules tended to attach themselves to the water surface, while the hydrophobic groups remained apart from the water surface.

Snapshots of energy-minimized configuration

The energy-minimized configurations of the dispersant molecules and those of their corresponding naked polar headgroups interacting with water surface (001) are shown in Figs. 3 and 4, respectively.

At the beginning of the dynamics process at 500 K, the dispersant molecules were placed on the water surface (001). Three of the dispersants, R-succinimide, R-acrylate and R-imide, showed similar dynamic behaviors in the MD simulations. Their configurations reached a stable state after 4 ps and their hydrophilic groups (strictly speaking, the electronegative atoms, such as oxygen and nitrogen) attached themselves to the water surface firmly. Their hydrophobic groups, *n*-octadecanyls, extended to the outside of the water surface. This situation corresponds closely to the realistic environment of dispersants when they interact with polar solid materials. The other two dispersants, R-phenylsulfonic and R-salicyl, shared a similar tendency of attaching their hydrophilic groups to the water surface, as compared to the above-mentioned three dispersants. However, it is difficult to change the angle of approximately 120° between *n*-octadecanyl and the phenyl ring due to the rigidity of the phenyl ring and the sp^3 hybridization of the benzene carbon. The configurations of these two dispersants can be seen as a balance between two opposite factors. One factor was that the hydrophilic groups moved towards the water surface due to the electrostatic attractive force and the hydrogen bond, the other factor was that the *n*-octadecanyl groups had the tendency to escape from the water surface. These two dispersants showed more intensive movements and swung on the water surface more than the other three dispersants did because of the rigidity of the dispersant molecules. This rigidity of the dispersant molecules played an important role in the interaction between the dispersants and the water surface. The more rigid the molecule was, the more intensive the movement.

MD simulations for the naked polar headgroups on water surface (001) were also performed in this study, showing that the naked polar headgroups moved more slowly than the dispersants because they tend to attach themselves more closely to the surface.

Compared to Figs. 3 and 4, it can be seen that the former three dispersants and their corresponding naked

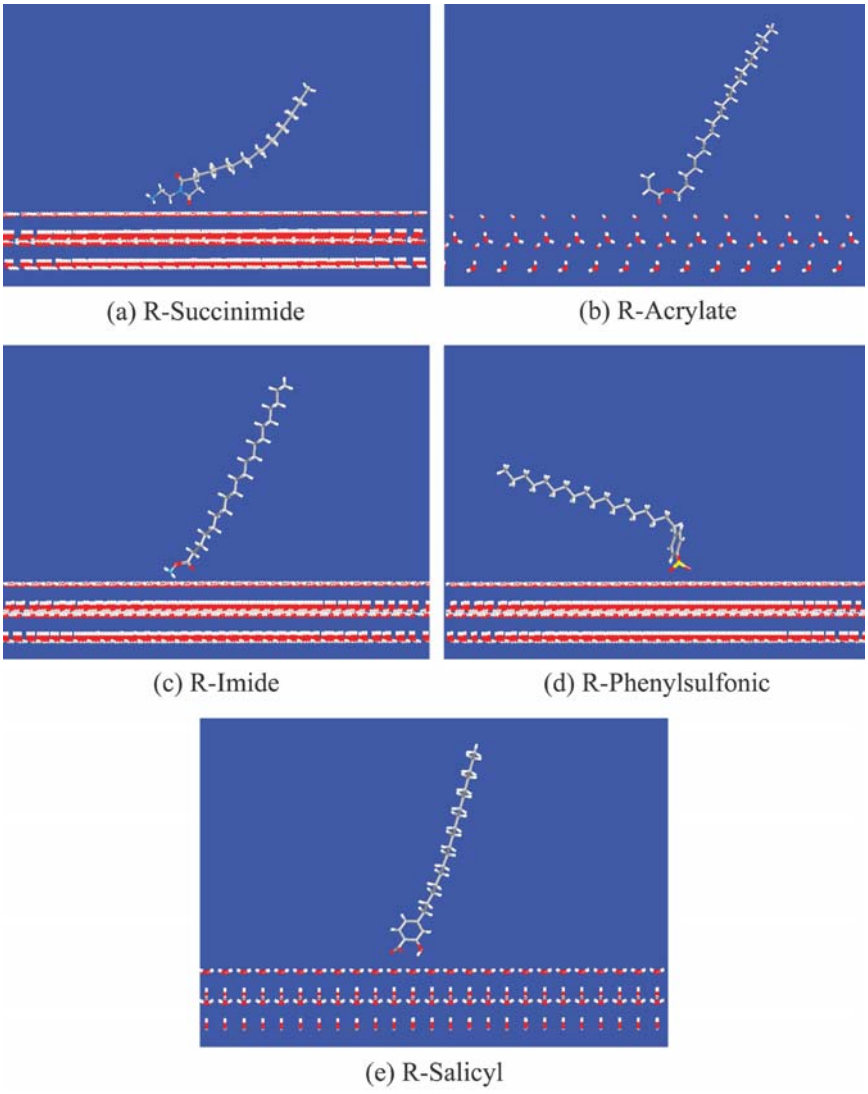

Fig. 3 Energy-minimized configurations of (**a**) R-succinimide, (**b**) R-acrylate, (**c**) R-imide, (**d**) R-phenylsulfonic, and (**e**) R-salicyl interacting with water surface (001)

polar headgroups showed nearly identical energy-minimized configurations. It is reasonable to say that the hydrophilic groups mostly induce their interface behavior when they interact with the water surface. However, the last two dispersants and their corresponding naked polar headgroups showed different energy-minimized configurations. These two dispersants attached themselves less closely to the water surface than their naked polar headgroups. This phenomenon was caused by the rigidity of the dispersant molecules arising from their inherent properties. The energy-minimized configurations of the dispersants on the water surface can be seen as the balance among their steric conformation, electrostatic factor and attractive or repulsive forces.

Energy analysis for the interaction between dispersants and water surface

In this study, the attachment energy of the dispersant molecule was defined as

$$E_{\text{attachment}} = E_{\text{dispersant+surface}} - E_{\text{dispersant}} - E_{\text{surface}} \quad (1)$$

where E_{surface} can be set to zero because the water molecules on the surface were kept unmoved during simulations, thus

$$E_{\text{attachment}} = E_{\text{dispersant+surface}} - E_{\text{dispersant}} \quad (2)$$

From the data presented in Tables 2 and 3, it can be found that the dispersants and their corresponding naked polar headgroups had negative values of the attachment energy. This mean that the total energy of the system would be reduced due to the interactions between the dispersants, or their naked polar headgroups, and the water surface.

When dispersants or their corresponding naked polar headgroups interacted with the water surface, the valence energy terms, as well as bonds, angle, torsion and inversion energies, were kept almost constant. On the contrary, the non-bond energy terms varied on a large scale, particularly the electrostatic and hydrogen bond energies.

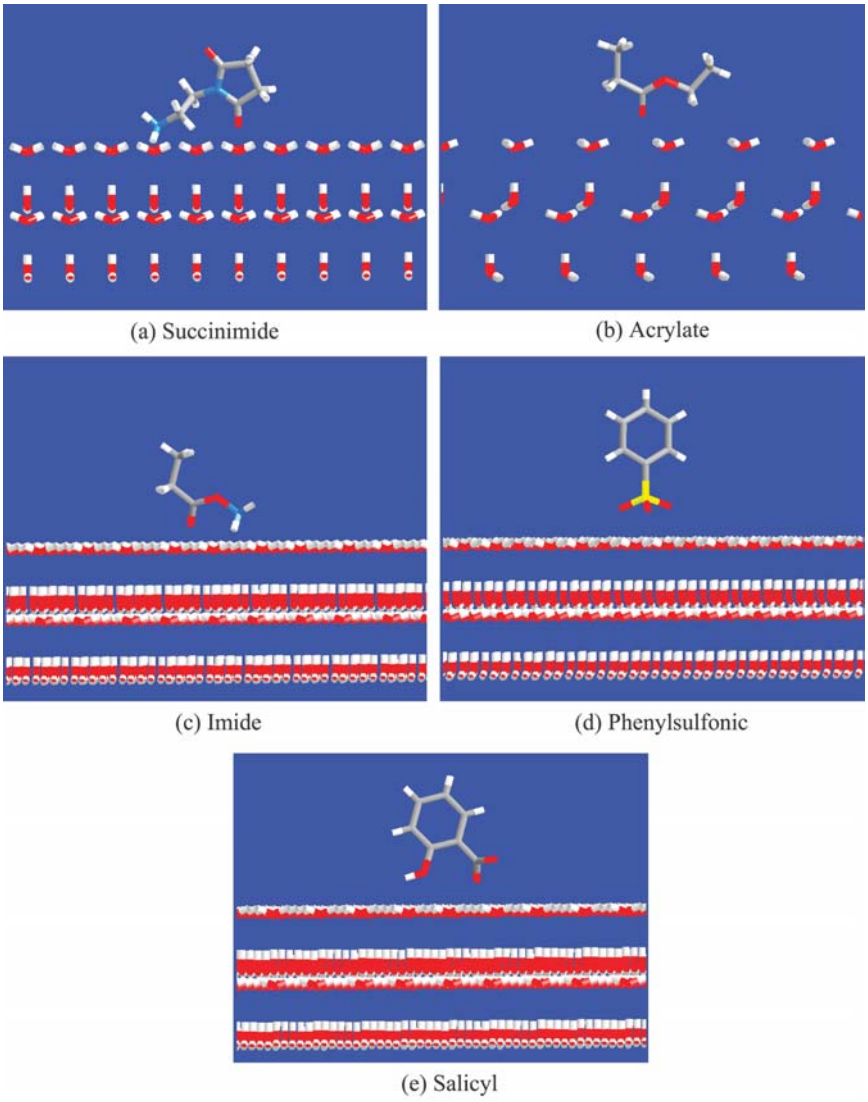

Fig. 4 Energy-minimized configurations of (**a**) succinimide, (**b**) acrylate, (**c**) imide, (**d**) phenylsulfonic, and (**e**) R-salicyl interacting with water surface (001)

Table 2 Decomposition energy terms listed for each R-substitute dispersant molecule interacting with the water surface

System	Total (kJ mol^{-1})	Valence (kJ mol^{-1})				Non-bond (kJ mol^{-1})		
		Bonds	Angles	Torsions	Inversions	van der Waals	Electrostatic	Hydrogen bonds
R-Succinimide+water surface	162.20	19.037	44.140	19.093	0.03966	161.52	−22.219	−59.405
R-Succinimide	249.69	19.024	44.870	9.904	0.03000	137.51	38.352	0.000
Attachment energy	−87.49	0.013	−0.730	9.187	0.00966	24.01	−60.571	−59.405
R-Acrylate+water surface	168.25	16.821	17.447	1.4661	0.09623	132.68	25.945	−26.208
R-Acrylate	224.06	16.508	15.967	0.7024	0.01506	129.65	61.216	0.000
Attachment energy	−55.81	0.313	1.480	0.7637	0.08117	3.03	−35.271	−26.208
R-Imide+water surface	167.64	17.097	19.254	1.7720	0.00084	145.26	25.603	−41.340
R-Imide	256.74	16.852	16.843	1.0753	0.00080	126.09	95.876	0.000
Attachment energy	−89.10	0.245	2.411	0.6967	0.00004	19.17	−70.273	−41.340
R-Phenylsulfonic+water surface	30.74	22.416	18.891	5.5379	0.10042	186.02	−167.67	−34.552
R-Phenylsulfonic	179.39	23.115	19.236	1.1140	0.00219	181.23	−42.824	−2.4887
Attachment energy	−148.65	−0.699	−0.345	4.4239	0.09823	4.79	−124.85	−32.063
R-Salicyl+water surface	214.54	21.228	136.99	11.709	0.18075	160.27	−91.168	−24.672
R-Salicyl	333.58	21.444	136.40	7.170	0.00594	156.91	11.659	0.000
Attachment energy	−119.04	−0.216	0.59	4.539	0.17481	3.36	−102.83	−24.672

Table 3 Decomposition energy terms listed for each naked polar headgroup of dispersant molecule interacting with the water surface

System	Total (kJ mol^{-1})	Valence (kJ mol^{-1})				Non-bond (kJ mol^{-1})		
		Bonds	Angles	Torsions	Inversions	van der Waals	Electrostatic	Hydrogen bonds
Succinimide+water surface	−31.579	3.4227	31.701	16.053	0.01527	44.278	−68.085	−58.963
Succinimide	42.100	3.2231	32.305	9.4171	0.00724	23.503	−26.356	0.000
Attachment energy	−73.679	0.1996	−0.604	6.6359	0.00803	20.775	−41.729	−58.963
Acrylate+water surface	−10.944	1.9193	8.8756	0.12761	0.00087	22.240	−18.006	−26.102
Acrylate	40.621	2.0498	7.9283	0.13891	0.01339	18.364	12.127	0.000
Attachment energy	−51.565	−0.131	0.9473	−0.01130	−0.01252	3.876	−30.133	−26.102
Imide+water surface	25.700	2.5519	7.3276	0.88584	0.00359	28.432	26.757	−40.258
Imide	98.944	2.2302	4.9670	0.18368	0.01887	11.960	79.584	0.000
Attachment energy	−73.244	0.3217	2.3606	0.70216	−0.01528	16.472	−52.827	−40.258
Phenylsulfonic+water surface	−73.234	8.0160	7.5607	4.0994	0.08368	77.840	−131.75	−39.081
Phenylsulfonic	104.01	8.1690	6.4803	5.4299	0.15732	59.035	24.734	0.000
Attachment energy	−177.24	−0.153	1.0804	−1.3305	−0.07364	18.805	−156.48	−39.081
Salicyl+water surface	41.348	5.2400	115.75	4.1155	0.00703	54.713	−115.83	−22.653
Salicyl	185.03	5.1700	115.90	4.1414	0.00435	45.520	14.298	0.000
Attachment energy	−143.68	0.0700	−0.15	−0.0259	0.00268	9.193	−130.13	−22.653

The energy due to van der Waals interaction force between the dispersant molecules, or their naked polar headgroups, and the water surface appeared as positive values, as shown in Tables 2 and 3. The van der Waals force represents non-bonded interactions between molecules. In this study, the van der Waals energy was calculated among the non-bonded atoms in a dispersant molecule or between the dispersant and water molecules with the Dreiding force field. A few water molecules within the van der Waals cut-off length were involved in the MD calculations for van der Waals energy when a dispersant molecule interacted with the water surface. Owing to the contributions from water molecules, the van der Waals energy of a dispersant molecule interacting with water molecules became larger than that of an isolated dispersant molecule. The dispersants R-succinimide and R-imide, and their corresponding succinimide and imide, had more atoms attached to the water surface as indicated by their energy-minimized configurations in Figs. 3 and 4. They had accordingly large van der Waals energy differences of 16.7–25.1 kJ mol^{-1}. However, the van der Waals energy differences of dispersant R-acrylate and its corresponding acrylate were less than 4.2 kJ mol^{-1} because they only had one oxygen atom attached closely to the water surface. For the dispersants R-phenylsulfonic and R-salicyl, the van der Waals energy differences were small, while their counterparts phenylsulfonic and salicyl had large values of the van der Waals energy differences of 8.4–18.8 kJ mol^{-1}. Comparing the energy-minimized configurations of these two dispersants with their naked polar headgroups on the water surface, more atoms such as SO_3^-, OH and COO^- attached themselves closely to the water surface in the case of the naked polar headgroups. This may be the reason that these two dispersants and their naked polar headgroups showed different van der Waals energies.

Owing to the contribution of electrostatic and hydrogen bond interactions, the dispersants can attach themselves firmly to the water surface, thus significantly reducing the energy of the system. In realistic lubricant oil systems, the dispersant molecules can attach themselves to polar solid materials and impede their further agglomeration.

Electrostatic interaction analysis

The hydrophilic groups of the dispersants, mainly comprising oxygen or nitrogen atoms, had more negative charge than the hydrophobic moieties. On the water surface (001), the hydrogen atoms with positive charge stretched to the upper side of the surface. The hydrophilic groups of the dispersants had a stronger tendency to attach themselves to the water surface than the hydrophobic groups. In contrast, the carbon atoms in the hydrophobic hydrocarbon chain had small values of negative charge, which were encompassed by the hydrogen atoms with positive charge. The hydrogen atoms in hydrophobic hydrocarbon chains played an important role in electrostatic interaction with the water surface. In other words, the tendency of the hydrophobic groups to escape from the water surface was due to the repulsive force between the hydrophobic groups and water surface. The charge distribution in dispersant molecules is shown in Table 4.

The differences of electrostatic energy for molecules originated from different situations. For the dispersants R-succinimide, R-acrylate and R-imide, their electrostatic energy differences were larger than those of the corresponding succinimide, acrylate and imide. The charge of oxygen or nitrogen in R-succinimide, R-acrylate and R-imide attached to the water surface became more negative than that in succinimide, acrylate and imide, as indicated in Table 4. The dispersant molecules can acquire larger electrostatic energy reduction than their corresponding naked polar headgroups when they interact with the water surface. However, the dispersants R-phenylsulfonic and R-salicyl showed inverse behavior of their electrostatic energy differences. The dispersant molecules acquired

Table 4 Charge distribution on dispersant molecules

Molecule	No.	Atom	Charge		No.	Atom	Charge	
			Dispersant	Naked polar headgroup			Dispersant	Naked polar headgroup
Succinimide	1	N	–0.6592	–0.6357	6	O	–0.5237	–0.4861
	2	C	–0.1808	–0.1747	7	C	–0.1296	–0.2449
	3	C	–0.1051	–0.1047	8	C	–0.2309	–0.2452
	4	N	–0.3641	–0.3630	9	C	+0.4397	+0.4589
	5	C	+0.4456	+0.4543	10	O	–0.5066	–0.4792
Acrylate	1	C	–0.4424	–0.4329	5	O	–0.5899	–0.5744
	2	C	–0.1966	–0.1967	6	C	+0.0095	+0.0117
	3	C	+0.6083	+0.6145	7	C	–0.2708	–0.3874
	4	O	–0.5168	–0.5039				
Imide	1	N	–0.4003	–0.3666	4	O	–0.5177	–0.4876
	2	O	–0.4899	–0.4785	5	C	–0.1953	–0.1983
	3	C	+0.6131	+0.6367	6	C	–0.3008	–0.4208
Phenylsul-fonic	1	O	–0.2906	–0.3284	6	C	–0.1139	–0.1078
	2	S	+0.0373	–0.0058	7	C	–0.1572	–0.1850
	3	O	–0.2996	–0.3346	8	C	+0.0276	–0.1490
	4	O	–0.2992	–0.3346	9	C	–0.1545	–0.1850
	5	C	+0.2749	+0.2910	10	C	–0.1151	–0.1078
Salicyl	1	O	–0.5436	–0.5911	6	O	–0.7040	–0.7358
	2	C	+0.6451	+0.6088	7	C	–0.1074	–0.1383
	3	O	–0.4476	–0.4942	8	C	+0.0137	–0.1857
	4	C	+0.0789	+0.0890	9	C	–0.1630	–0.1910
	5	C	+0.2525	+0.2648	10	C	–0.2009	–0.1965

lower electrostatic energy reduction than their corresponding naked polar headgroups primarily due to their adverse charge variation.

These electrostatic energy differences induced by the hydrophobic moieties became less important and conspicuous when their hydrocarbon chains became longer. In realistic dispersant molecules, longer hydrophobic hydrocarbon chains are required, the molar mass of which may exceed ten thousand, and this influence will become less significant. We note that the influence arising from the hydrophobic hydrocarbon chain should be taken into consideration when designing new dispersants.

Hydrogen bond interaction and RDF analysis

Tables 2 and 3 show that there is hardly any difference in the hydrogen bond energy between dispersants and their corresponding naked polar headgroups. This is reasonable because the hydrogen bond energy is related to specific atoms, such as oxygen and nitrogen, in the hydrophilic groups and not directly to the hydrophobic hydrocarbon chains. The MD simulation results in this work confirm this characteristic. The dispersants R-succinimide, R-phenylsulfonic and R-imide gained larger hydrogen bond energy reduction because there are more atoms that can form hydrogen bonds in these dispersant molecules than in the others. For the dispersant R-salicyl, the charge of the oxygen atoms was low, although there are three oxygen atoms available to form hydrogen bonds. This dispersant therefore has a greater potential to escape from the water surface than the others due to the electrostatic interaction. In other words, longer distances are found between the oxygen atoms and the water surface. The difference in the distance between the hydrophilic group and the water surface can be seen in the energy-minimized configuration in Fig. 4e. The hydrophobic hydrocarbon chains directly influence the movement of the hydrophilic groups in changing the distance between the hydrophilic groups and the water surface, which indirectly affects the hydrogen bond energy. Thus, when hydrophilic groups can attach themselves firmly to the water surface, small differences of the hydrogen bond energy should exist between the dispersants and their naked polar headgroups. As indicated by the data in Tables 2 and 3, the difference in hydrogen bond energy between the first three dispersants and their corresponding naked polar headgroups is less than 1.26 kJ mol^{-1}, while larger difference of 2.1–7.1 kJ mol^{-1} are found between the last two dispersants and their corresponding naked polar headgroups.

The radial distribution function (RDF) curves were analyzed for the dispersant molecules in order to examine the role of hydrogen bond in the dynamic process.

For dispersant R-succinimide and its counterpart succinimide, the RDF curve of O_2 and H___A shows a sharp peak at ~2 Å in Fig. 5, indicating that a strong hydrogen bond forms between the oxygen atom in the carboxyl group and the hydrogen atom on the water surface. Other peaks appeared in the RDF curve of O_2 and H___A at longer distances because of the periodic distribution of water molecules in space. Two hydrogen atoms with the H___A force field type existed in the hydrophilic group of succinimide. It can be seen that an

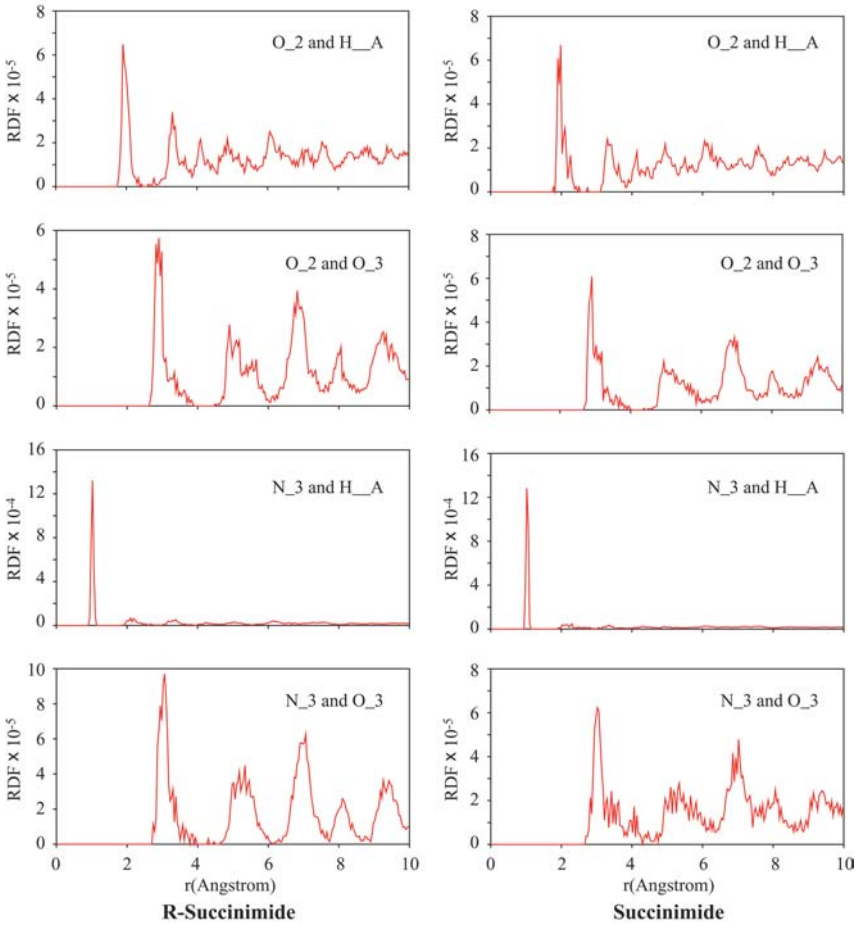

Fig. 5 RDF curves for R-succinimide and succinimide

intensive peak appeared at ~3 Å in the RDF curve of O_2 and O_3, where O_2 and O_3 were related to the oxygen atoms in the carboxyl group and in water, respectively. Since there are twice as many hydrogen atoms as oxygen atoms on the water surface, the number of peaks in the RDF curve of O_2 and H___A was nearly twice of that of O_2 and O_3. For the nitrogen atom in the amine, an intensive peak appeared at ~1 Å (this distance is approximately equal to the bond length between nitrogen and hydrogen atoms) in the RDF curve of N_3 and H___A, because of the two hydrogen atoms connected to the nitrogen atom in the amine. The inconspicuous peak at ~2 Å corresponded to the hydrogen bond formed between the nitrogen in the amine and hydrogen atoms in water. The other inconspicuous peaks that appeared in the RDF curve of N_3 and H___A were the results of the periodic space distribution of water molecules. For these peaks, the hydrogen bond becomes weak or dies out at longer distances. The RDF curves of N_3 and O_3 also indicated the existence of hydrogen bonds below 3 Å, in a manner similar to the RDF curve of O_2 and O_3. It was evident from the RDF curves that a hydrogen bond exists between the oxygen atom in the carboxyl group and the hydrogen atom in water, or between the nitrogen atom in the amine and the hydrogen atom in water.

For dispersant R-acrylate and its counterpart acrylate, both of the oxygen atoms in the hydrophilic group can form hydrogen bonds with the water surface. The sharp peak in the RDF curve of O_2 and H___A in Fig. 6 shows that a hydrogen bond forms at ~2 Å between the oxygen atom in the carboxyl group and the hydrogen atom of water. In the RDF curve of O_R and H___A, a rough and broad peak appeared at 3–4 Å, indicating a weak interaction between the oxygen atom in the ester group and the hydrogen atom in water. The oxygen atom in the ester group can leave the water surface, as can be easily found in the energy-minimized configurations of R-acrylate and acrylate interacting with the water surface in Figs. 3b and 4b, respectively.

Similar to the discussions on the dispersant R-succinimide, the RDF curve for the dispersant R-imide showed almost identical results. The curves in Fig. 7 also confirmed that the oxygen atom in the carboxyl group and the nitrogen atom in the amine can form hydrogen bonds at ~2 Å with the hydrogen in water surface.

The RDF curves for the dispersant R-phenylsulfonic in Fig. 8 indicate that the oxygen atom in sulfite can form hydrogen bonds at ~2 Å with the hydrogen on the water surface. However, the intensity of the peak at ~2 Å for phenylsulfonic was lower than that of R-phenylsulfonic. The R-phenylsulfonic molecule is more rigid than

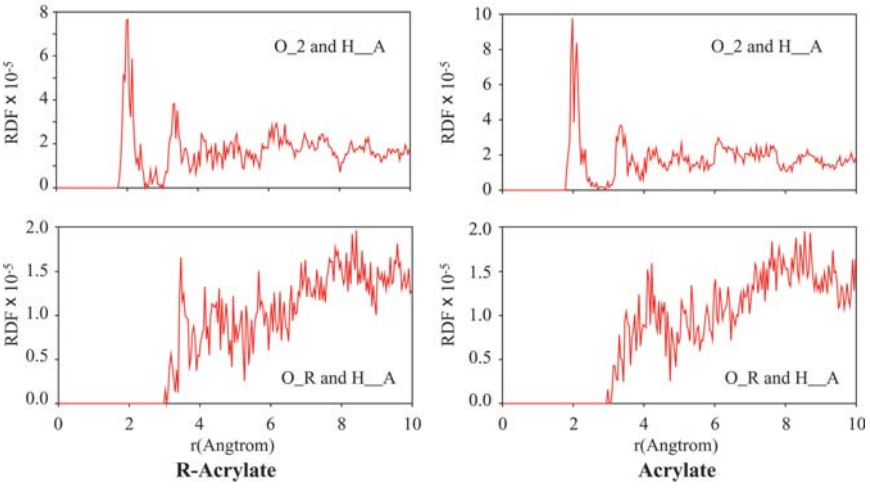

Fig. 6 RDF curves for R-acrylate and acrylate

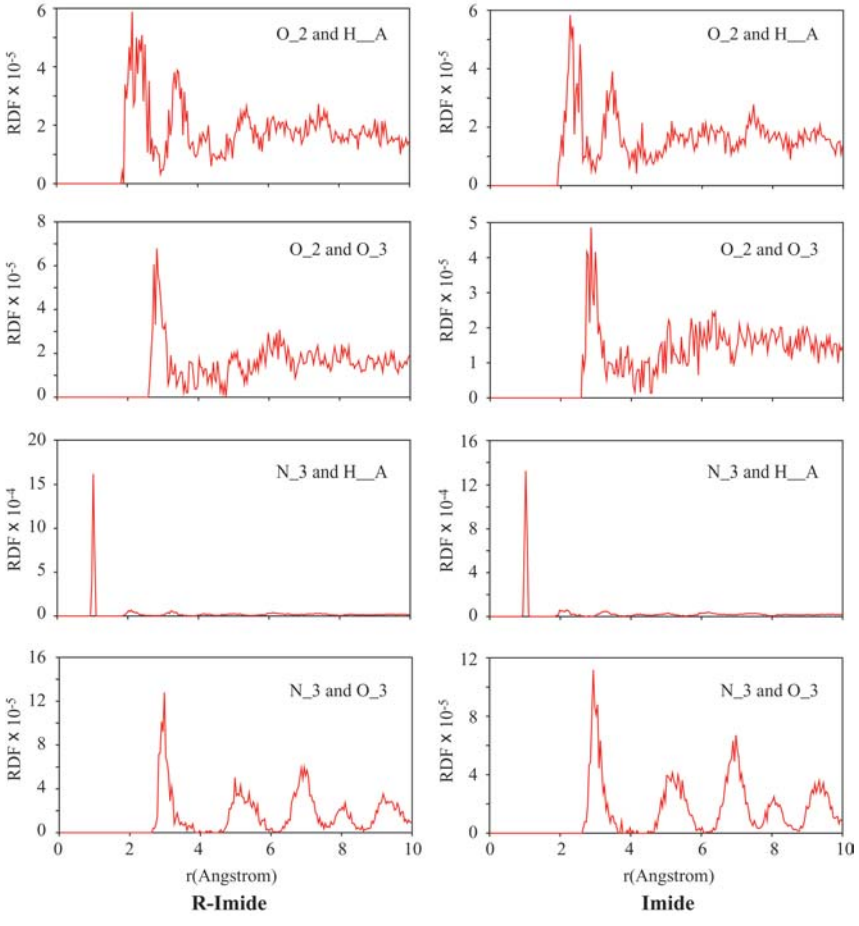

Fig. 7 RDF curves for R-imide and imide

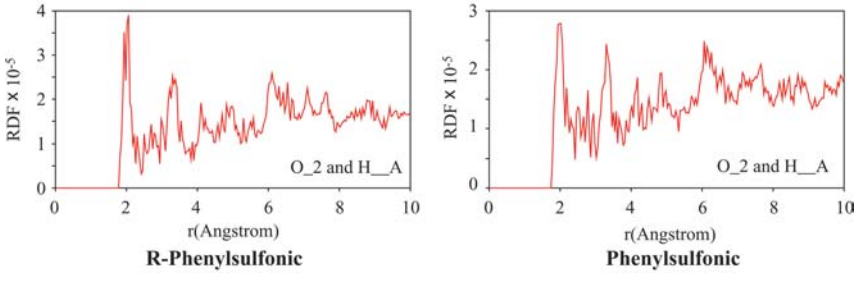

Fig. 8 RDF curves for R-phenylsulfonic and phenylsulfonic

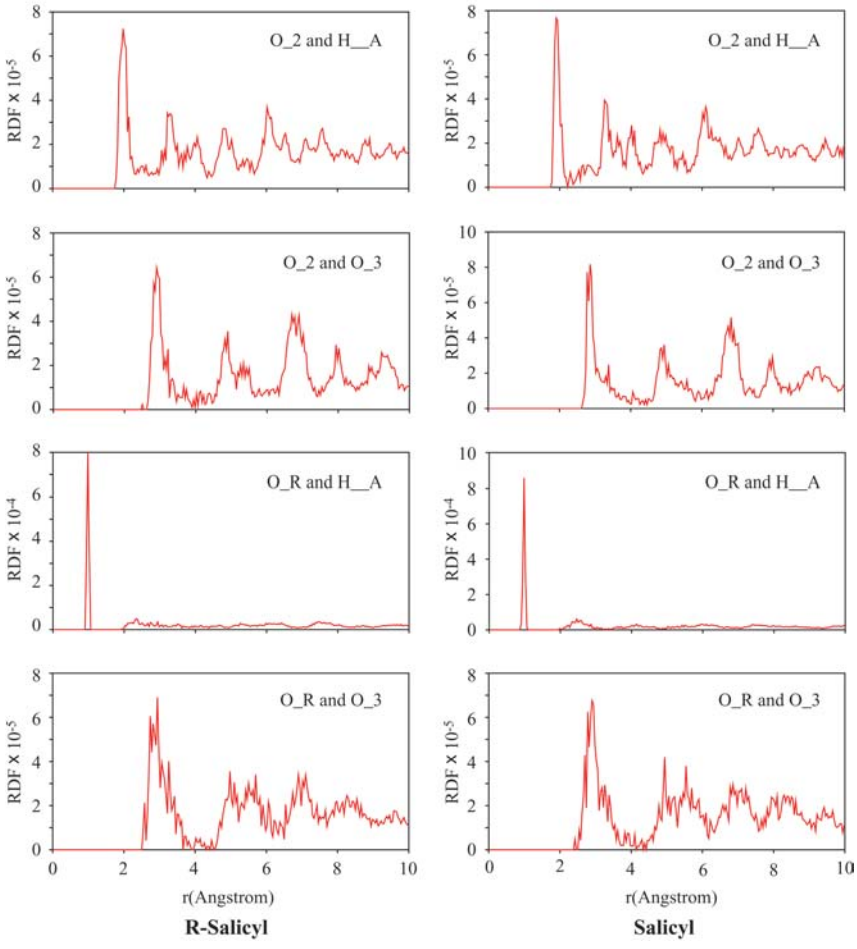

Fig. 9 RDF curves for R-salicyl and salicyl

phenylsulfonic, and the movement of the R-phenylsulfonic molecule was violent on the water surface. In comparison with the dispersant R-phenylsulfonic, the three oxygen atoms in phenylsulfonic have well-ordered fixed distances from the hydrogen atoms in the water surface, thus causing the homogenization of the peaks in the RDF curve. Thus, the most intensive peak for phenylsulfonic must be lower than that for R-phenylsulfonic.

For dispersant R-salicyl and its corresponding salicyl, the RDF curves in Fig. 9 also confirm that the oxygen atoms in the hydroxyl group and the carboxyl group can form hydrogen bonds with hydrogen atoms on the water surface at ~2 Å and 2–3 Å, respectively. Salicyl showed higher peak intensity than R-salicyl, as is obvious in the RDF curve of O_R and H___A at 2–3 Å. The oxygen atoms in salicyl have well-ordered fixed distances from the hydrogen atoms on the water surface as compared to those in R-salicyl, because the R-salicyl molecule is more rigid than salicyl and the movement of R-salicyl was violent on the water surface. Thus, salicyl showed higher peak intensity.

The van der Waals radii of oxygen, nitrogen and hydrogen atoms, obtained from the Dreiding 2.21 force field, are 1.520 Å, 1.550 Å and 1.200 Å, respectively. The van der Waals radius sum of O–H and N–H are thus 2.720 Å and 2.750 Å, respectively. The covalent bond lengths in O–H and N–H are also estimated to be 0.947 Å and 1.025 Å, respectively. It can be seen from the above discussions that a stable hydrogen bond existed between the oxygen (or nitrogen) atom and the hydrogen atom on the water surface. The length of the hydrogen bonds was larger than the corresponding covalent bonds, but less than their corresponding van der Waals radius sum.

Conclusions

The models of the dispersants and the polar water surface were built in order to study their interactions, which are important to the dispersants' dispersancy. It can be seen from the MM and MD simulations that electrostatic and hydrogen bond energies play important roles in the stabilization of the system comprising dispersant molecules and the polar water surface. Simulation results are found to be consistent with observed phenomena in experiments.

The hydrophilic groups of carboxylic, hydroxyl and amide in the dispersant molecules attach themselves firmly to the water surface and reach for the stable

energy-minimized configurations. These groups possessed strong potentials to form hydrogen bonds. Due to their electrostatic and hydrogen bond interactions, the dispersant molecules tend to physisorb on the surface of the polar materials and reduce the total energy of the system. Such interactions were influenced by steric configuration, charge distribution and substituents of the dispersant molecules.

Further studies on solvent effect and micelle phenomena are still required for detailed discussions on the mechanism of dispersancy.

Acknowledgements The authors are grateful to professor Mooson Kwauk of Institute of Process Engineering for his revision of the manuscript, Dr. Xiao-Hui Mu, Xiao-Guang Zhao and Zhen-Yu Dai of SINOPEC for their helpful discussions.

References

1. Tomlinson A, Danks TN, Heyes DM (1997) Langmuir 13:5881–5893
2. Cox AR, Vincent B, Harley S, Taylor SE (1999) Colloids Surf, A, Physicochemi Eng Aspects 146:153–162
3. Tomlinson A, Scherer B, Karakosta E, Oakey M, Danks TN, Heyes DM, Taylor SE (2000) Carbon 38:13–48
4. Pugh RJ, Matsunaga T, Fowkes FM (1983) Colloids Surf 7:183–207
5. Pugh RJ, Fowkes FM (1984) Colloids Surf 9:33–46
6. de Sainte Claire P, Hass KC, Schnerder WF, Hase WL (1997) J Chem Phys 106:7331–7342
7. Manunzaa B, Deianaa S, Pintorea M, Gessab C (1997) J Mol Struct (Theochem) 419:133–137
8. Toxvaerd S (2000) J Mol Liq 84:99–110
9. Hentschke R, Schürmann BL, Rabe JP (1992) J Chem Phys 96:6213–6221
10. Böcker J, Gurskii Z, Heinzinger K (1996) J Phys Chem 100:14969–14977
11. Ge Q, Hu P, King DA, Lee M-H, White JA, Payne MC (1997) J Chem Phys 106:1210–1215
12. Boop PA, Heinzinger K (1998) J Electroanal Chem 450:165–173
13. Michael D, Benjamin I (1998) J Electroanal Chem 450:335–345
14. Fernandes PA, Cordeiro MNDS, Gomes JANF (1999) J Mol Struct (Theochem) 463:151–156
15. ter Horst JH, Wong Fong Sang KE, de Vreugd CH, Geertman RM, Witkamp GJ, van Rosmalen GM (1999) Colloids Surf, A, Physicochem Eng Aspects 154:273–284
16. Boeyens JCA, Comba P (2001) Coord Chem Rev 212:3–10
17. Bartha L, Deák G, Hancsók J, Auer J, Kocsis Z (2001) Lubr Sci 13:313–327
18. Bezot P, Hesse-Bezot C, Diraison C (2001) Lubr Sci 13:301–311